Plasmonic metal–dielectric–metal stack structure with subwavelength metallic gratings for improving sensor sensitivity and signal quality

Sherif H. El-Gohary, Jong Min Choi, Nak-Hyeon Kim, and Kyung Min Byun*

Department of Biomedical Engineering, Kyung Hee University, Yongin 446-701, South Korea

*Corresponding author: kmbyun@khu.ac.kr

Received 13 December 2013; revised 13 February 2014; accepted 26 February 2014;
posted 28 February 2014 (Doc. ID 202989); published 28 March 2014

In this study, we investigated the performance improvement of a localized surface plasmon resonance (LSPR) biosensor by incorporating a metal–dielectric–metal (MDM) stack structure and subwavelength metallic nanograting. The numerical results showed that the LSPR substrate with a MDM stack can provide not only a better sensitivity by more than five times but also a notably improved signal quality. While the gold nanogratings on a gold film inevitably lead to a broad and shallow reflectance curve, the presence of a MDM stack can prevent propagating surface plasmons from interference by locally enhanced fields excited at the gold nanogratings, finally resulting in a strong and deep absorption band at resonance. Therefore, the proposed LSPR structure could potentially open a new possibility of enhanced detection for monitoring biomolecular interactions of very low molecular weights. © 2014 Optical Society of America

OCIS codes: (240.6680) Surface plasmons; (310.6628) Subwavelength structures, nanostructures; (280.1415) Biological sensing and sensors.

http://dx.doi.org/10.1364/AO.53.002152

1. Introduction

The surface plasmon resonance (SPR) technique has been extensively used in monitoring chemical and biological reactions due to its advantages such as real-time, label-free, and quantitative detection. A SPR-based biosensor detects the integral change in the dielectric medium in the vicinity of a metal film. Contrary to a planar metal film where the surface plasmon (SP) fields penetrate into the dielectric ambient up to several hundred nanometers, metallic nanostructures make the plasmon field highly confined to the surface [1]. As a strong confinement of localized surface plasmons (LSPs) can promote plasmonic interaction with target analytes and efficient transduction of surface binding events, an improved sensitivity has been achieved by overlapping the localized field with bound target analytes [2]. In our previous investigations, the use of periodic metallic nanogratings built on a thin metal film resulted in a significant SPR signal amplification [3].

Despite such advantages concerning the sensitivity, several adverse effects associated with metallic nanostructures have not been fully addressed yet. It has been found that the metallic nanostructures directly deposited on a thin metal film make the SPR curve significantly broader and shallower, which is attributable to the simultaneous excitation of propagating and localized plasmon modes. When the nanostructure size is increased, multiple localized surface plasmon resonances (LSPRs) are produced prominently and lead to a damping of SP waves through a destructive coupling between them [4]. The weak and shallow absorption bands of a SPR curve can increase the uncertainty of the sensor

1559-128X/14/102152-06$15.00/0

output and affect a high standard error in experimental measurement, producing a notable degradation of the sensor performance.

Hence, in order to separate the LSP modes from the propagating SP waves, different plasmonic structures have been suggested while maintaining the benefit of a sensitivity improvement. For example, nanoparticle-embedded dielectric coating on a thin gold film showed a significant sensitivity enhancement by more than 10 times [5]. Compared to the previous approach of immobilizing gold nanoparticles directly on a thin gold film by drying a chemical solution containing suspended gold nanoparticles, which often suffered from the difficulties in controlling the volume fraction of the nanoparticles, an alternative fabrication method of an RF magnetron cosputtering process allowed gold nanoparticles embedded in the dielectric film to be apart from a gold film. Similarly, the application of dielectric–metal double-layered nanogratings to a gold film was explored theoretically [4]. The dielectric spacer between a gold film and a gold nanograting could prevent the propagating SPs from interference by the locally enhanced fields. As a result, the double-layered dielectric–metal gratings provided 10-fold enhancement in sensitivity and better signal quality in comparison with single-layered gold nanogratings. However, in those cases, as the resonance angle is found in a higher momentum, the system has a very narrow dynamic range and thus still remains challenging in actual applications.

In this work, we demonstrate SPR signal enhancement by incorporating multiple planar films and periodic metallic nanogratings. A multilayer consisting of a metal–dielectric–metal (MDM) stack works as a kind of waveguide structure. From in-depth design study on geometric parameters of MDM and gold nanogratings, improved sensing properties such as higher sensitivity and better signal quality will be presented. Such enhancement is possibly due to the advantages of the plasmonic waveguide structure, i.e., longer propagation length and higher subwavelength mode confinement [6]. The proposed configuration could be an interesting alternative to the application of realizing high-sensitivity sensors, nanoscale photonic circuits, and photonic devices.

2. Numerical Model

Figure 1 shows a schematic diagram of the proposed LSPR biosensor. A thin gold film with a thickness of 45 nm is coated on a SF10 glass substrate via attachment of a 2-nm-thick chromium layer. The MDM stack structure consists of a 45-nm-thick gold film, a SiO_2 layer, and a gold overlayer. The thicknesses of the dielectric film and gold overlayer are denoted as d_D and d_{OL}. One-dimensional rectangular grating with a period of $\Lambda = 100$ nm, a width of 50 nm (i.e., a fill factor $f = 0.5$), and a thickness of 20 nm is regularly patterned on the MDM-stack-mediated plasmonic substrate. The period of 100 nm is chosen based on our previous studies, demonstrating that an

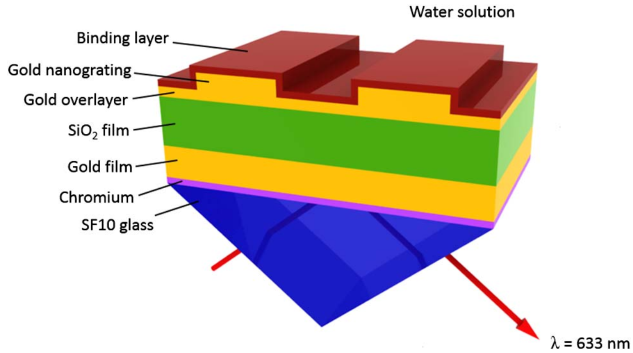

Fig. 1. Schematic of the proposed LSPR substrate with MDM stack structure and gold nanogratings. TM-polarized light with $\lambda = 633$ nm propagating into an SF10 glass prism is incident to the LSPR configuration with an adhesion layer of chromium (2 nm), a thin gold film (45 nm), SiO_2 dielectric film (d_D), a gold overlayer (d_{OL}), and gold nanogratings (20 nm). Rectangular gold nanogratings of a period of $\Lambda = 100$ nm and a width of 50 nm are regularly patterned on a planar stack structure. A 2-nm-thick binding layer is assumed to cover the whole substrate surface uniformly.

extremely sensitive LSPR structure typically requires metallic gratings of sub-50-nm linewidth, while the difficulty in an actual fabrication may increase [3,7]. Note that use of an adhesion between SiO_2 film and gold overlayer is not considered here for fair comparison with other plasmonic substrates such as thin gold films with and without gold nanogratings. A binding event occurring at the grating surface is modeled as a 2-nm-thick dielectric layer that covers the whole sensor surface uniformly. The refractive index of the binding layer (n_{BL}) is set to be 1.40 for ligand immobilization and increases up to 1.50 according to an interaction between capture and target probes. This refractive index change is based on the measurement data obtained from ellipsometric characterizations for DNA hybridization [8]. TM-polarized light at the wavelength $\lambda = 633$ nm is incident to the substrate. The optical constants $\varepsilon = (n, k)$ of SF10 substrate, chromium, and gold are set to be (1.723, 0), (4.30, 4.96), and (0.122, 3.110), respectively, at $\lambda = 633$ nm [9]. Also, the refractive indices of SiO_2 and water solution are assumed to be 1.457 and 1.330.

For numerical simulations, we employ a rigorous-coupled-wave analysis (RCWA) method, which has been successfully used to explain the experimental results of grating structures [10,11]. Based on the previous work, our RCWA routine was proved to corroborate the experiments of earlier SPR and LSPR studies based on dielectric and metallic nanostructures. Note that, since the field varies more rapidly in short distances of a grating with size smaller than a wavelength λ, more space-harmonic orders are required to achieve the convergence and to improve the accuracy in calculations [12], and 30 spatial harmonics have been considered. The reflectance curve is obtained from RCWA calculations as the light incidence is scanned with an angular resolution of

0.01°. As a quantitative measure of the sensitivity improvement, we employ a sensitivity enhancement factor (SEF), which is the ratio of the SPR angle shift due to an increasing n_{BL} of the binding layer on LSPR substrates to that of a conventional SPR structure. While SPR curves are not shown for a conventional SPR system, the resonance angles are 59.45° for $n_{BL} = 1.40$ and 59.63° for $n_{BL} = 1.50$ in water solution; thus, the reference SPR shift is 0.18°.

3. Results and Discussion

A. Effect of SiO_2 Thickness on SPR Sensor Performance

As a dielectric film plays an important role in blocking direct coupling of localized and propagating SPs at the interface of gold film and gold nanograting, we investigate the effect of dielectric film thickness on the SPR characteristics as a first step. In this calculation, the gold overlayer is not taken into consideration, and the geometry of gold nanogratings is fixed at a period of $\Lambda = 100$ nm and a thickness of 20 nm. Figure 2 presents the SPR curves when the SiO_2 film thickness d_D increases from 0 to 200 nm. Note that minimum reflectance values at resonance are larger than 0.4 at the SiO_2 thickness of $d_D < 100$ nm. Such a shallow SPR dip is practically inappropriate for accurate detection of binding events. Also, since minimum reflectance is associated with the sensing contrast (i.e., the signal-to-noise ratio), smaller minimum reflectance values are required, and we find a remarkable reduction of minimum reflectance at the range of $d_D \geq 120$ nm. At this range, the resonance angle tends to decrease gradually, which means that the dynamic range in measurement is increased.

In Fig. 3, the substrates with a dielectric spacer provide a significant improvement of sensitivity at a wide thickness ranging from 110 nm $\leq d_D \leq$ 150 nm, implying performance reliability and robustness to fabrication errors in implementing the plasmonic platform. The dotted line represents the SPR shift of 0.18° for a conventional SPR structure. The maximum SEF is obtained to be 2.6 at $d_D = 120$ nm. On the other hand, it is interesting to find in Fig. 3 that, when the dielectric layer thickness is increased, the SEF reaches a maximum of 0.47° and then starts to decrease. Continuing reduction of SEF can be explained by the limited penetration depth of plasmon waves with rapidly decaying intensity when one moves away from the metal surface. Since the detection range of the SPR biosensor is intrinsically confined to the penetration depth with a dimension of several hundred nanometers, an increasing d_D over the plasmon decay length may not contribute to the sensitivity enhancement, finally leading to a degraded performance lower than that of a conventional SPR system. As a result, a reasonable thickness range of the SiO_2 film should be less than 150 nm.

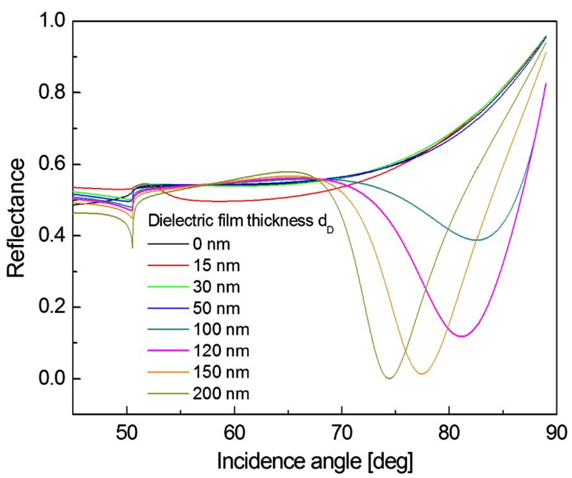

Fig. 2. SPR curves of the LSPR substrate without a gold overlayer as the thickness of SiO_2 film varies from 0 to 200 nm.

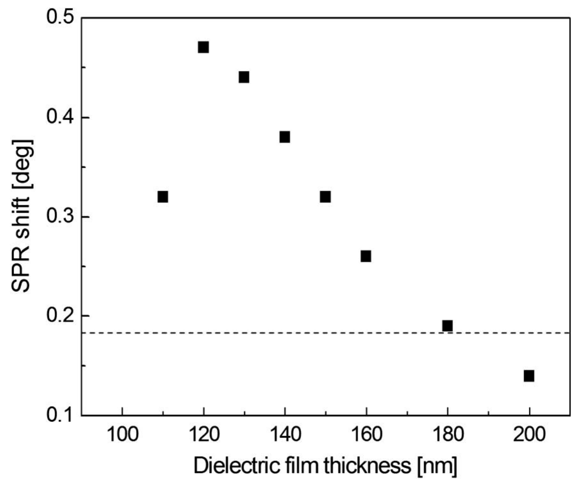

Fig. 3. Sensitivity characteristics of the LSPR substrate without a gold overlayer with respect to the dielectric film thickness. The dotted line indicates the sensitivity of a conventional SPR system.

B. Effect of Gold Overlayer Thickness on SPR Sensor Performance

Although introduction of a dielectric layer is an effective method for improving the SPR signal quality of a nanograting-mediated LSPR system, the sensor sensitivity is still not satisfactory. Closely spaced gold nanogratings with a period less than 100 nm can provide a notably enhanced sensitivity gain due to a better field-analyte interaction by increased surface reaction area and enhanced local plasmon field. However, the difficulties in the actual fabrication of densely packed gratings make the realization of a highly sensitive plasmonic substrate infeasible. Instead, we intend to add a thin gold overlayer on the dielectric film, as it is well known that the MDM stack structure is advantageous in sensing applications, which is primarily on account of a longer propagation length and higher subwavelength mode confinement. Therefore, we hypothesize that by coating a SiO_2 film with a gold overlayer, plasmonic fields can interact with the target samples more efficiently, and thus the sensitivity will be increased significantly.

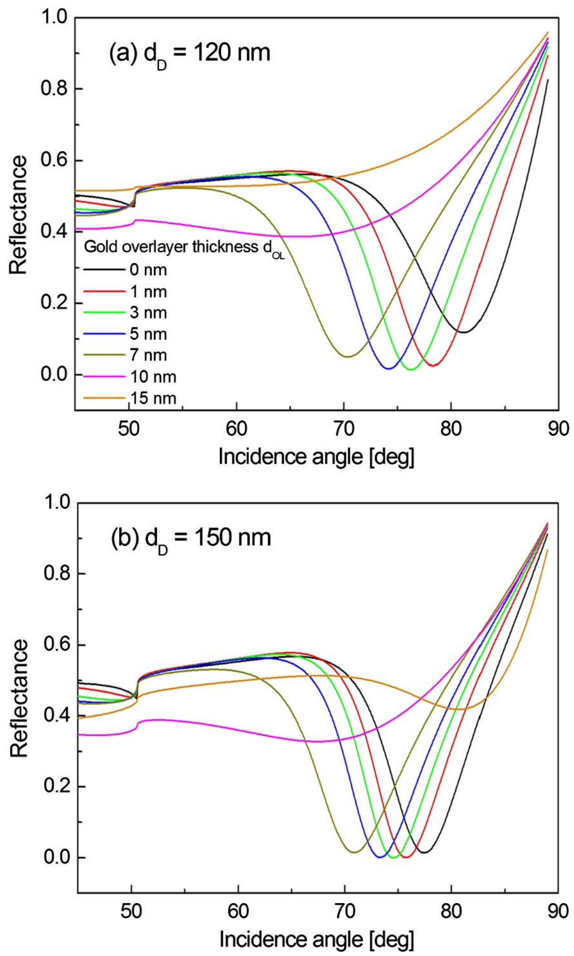

Fig. 4. SPR curves of the proposed LSPR substrate when the thickness of the gold overlayer increases from 0 to 15 nm. SiO_2 dielectric film has a thickness of (a) 120 nm and (b) 150 nm, respectively.

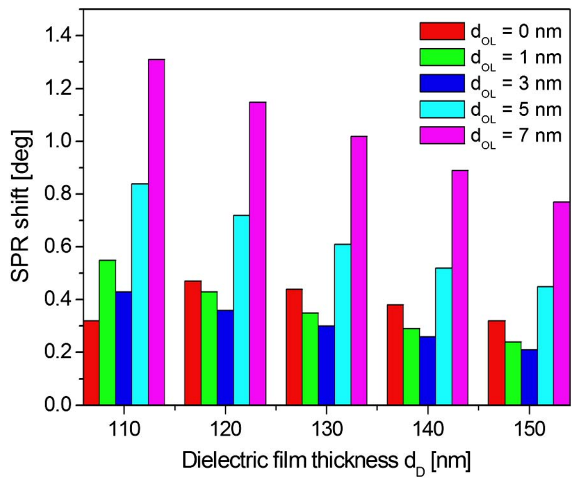

Fig. 5. Sensitivity characteristics of the LSPR substrate with respect to the thicknesses of the dielectric film and gold overlayer. The geometry of rectangular gold nanogratings is fixed at a period of $\Lambda = 100$ nm, a width of 50 nm, and a thickness of 20 nm.

Figure 4 shows the effect of a gold overlayer with a thickness d_{OL} from 0 to 15 nm for LSPR structures of $d_D = 120$ and 150 nm. Obviously, there is an observation that the resonance shifts toward a smaller angle gradually in accordance with an increase in d_{OL} ranging from 0 to 7 nm. Such a lower SPR angle allows a convenient measure in angle-scanning experiments as well as a large dynamic range. On the other hand, a substantial increase of minimum reflectance is found at the d_{OL} thicker than 7 nm. This supports the assertion that while the SPR characteristics can be improved by inserting a gold overlayer, selecting a gold film of a thickness less than 10 nm would be suitable for accurate detection of binding events.

As a next step, we consider the sensor sensitivity by varying the thickness of the gold overlayer. Figure 5 plots the SPR shift with respect to a gold overlayer thickness for different dielectric film geometries. Note that the sensitivity values for SPR curves with a minimum reflectance > 0.3 are not shown because a shallow SPR dip is practically improper for efficient biosensing. Compared with the cases without a gold overlayer, notable increment in sensitivity is accomplished when d_{OL} is larger than 5 nm. In particular, $d_{OL} = 7$ nm exhibits the highest sensitivity for the whole cases, and the maximum SEF value of 7.3 is obtained at $d_D = 110$ nm. It is also interesting to find that the SPR shift is decreased with an increasing d_D when d_{OL} is fixed, which is attributable to the penetration depth of SPs.

Based on the quantitative metrics of SEF, minimum reflectance, and dynamic range, the optimal design parameters of the proposed LSPR substrate are determined to be a SiO_2 film thickness in the range of 110 nm $\leq d_D \leq$ 150 nm and a gold overlayer with a thickness of $d_{OL} = 7$ nm. This geometry results in not only a significantly enhanced sensitivity more than five times larger than that of a conventional SPR biosensor, but also a strong absorption band and a large dynamic range.

C. Effect of Chromium Thickness on SPR Sensor Performance

In the fabrication process of the designed plasmonic platform, the thickness control of the chromium adhesion layer is another important issue for successful realization of the LSPR samples. Thin transition metal films, such as chromium, titanium, and tungsten, are generally employed as adhesion promoters between a noble metal film and a glass substrate [13]. They have been frequently used to improve the adhesion and to enhance the stability of the noble metal film. If the adhesion film is not used, the metal film supporting plasmon excitation can be peeled off or damaged by severe processes, such as oxidation and dry etching and/or subsequent SPR experiments. In this section, the influence of the thickness of chromium adhesion film on the sensor performance will be briefly explored.

When the thicknesses of the SiO_2 film and gold overlayer are, respectively, set to be 150 and 7 nm, Fig. 6 presents that the sensitivity decreases considerably as the thickness of the chromium layer

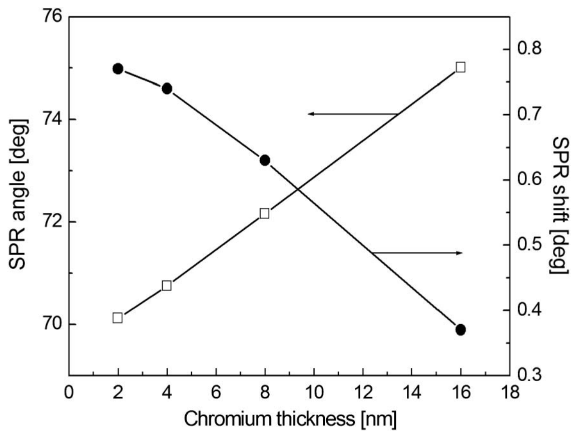

Fig. 6. Sensor performance of SPR angle and its shift as the thickness of chromium film increases from 2 to 16 nm. The thicknesses of SiO_2 film and gold overlayer are set to be $d_D = 150$ nm and $d_{OL} = 7$ nm.

increases up to 16 nm. Moreover, when a thick adhesion is employed, the chromium layer makes the resonance angle shifted to a higher momentum and leads to a limited dynamic range. Although the negative contribution of the chromium becomes stronger as its thickness increases, trade-off analysis on the optimal chromium thickness is essential for achieving good sensing characteristics and robust SPR substrates. Judging from an abrupt drop of the sensitivity in Fig. 6, the maximally allowable thickness of the chromium layer should not exceed 5 nm in actual fabrication.

D. Near-Field Characteristics

In order to verify the effect of the SiO_2 film and gold overlayer, we visualize the enhanced plasmon fields near the sensor surface using the finite-difference time-domain (FDTD) method. From FDTD calculation, a two-dimensional distribution of near-field intensity on the sensor surface is visualized to estimate the field enhancement of LSP modes quantitatively. The minimum grid size is set to be 0.5 nm. We have chosen the LSPR substrate with SiO_2 film at $d_D = 120$ nm, gold overlayer at $d_{OL} = 5$ nm, and a 2-nm-thick chromium layer. A resonance angle of 74.21° is used as the incidence condition of a monochromatic light at $\lambda = 633$ nm.

In Fig. 7, the field distribution of E_x exhibits well-known features of LSP modes excited by gold nanogratings. Locally enhanced fields are distributed at a very short distance from the surface in the vicinity of grating vertices. Also, there are multiple peaks at each corner of the gold nanograting. On the assumption that the electric field of an incident beam is of unit amplitude, the maximum field amplitude is obtained as $E_x = 144.4$ for $d_{OL} = 5$ nm. While the results for $d_{OL} = 0$ nm are not shown here, the LSPR substrate with no gold overlayer produces a peak value of $E_X = 82.4$. This supports that, in the presence of a gold overlayer, the plasmon fields are more efficiently confined to the sensor surface, which

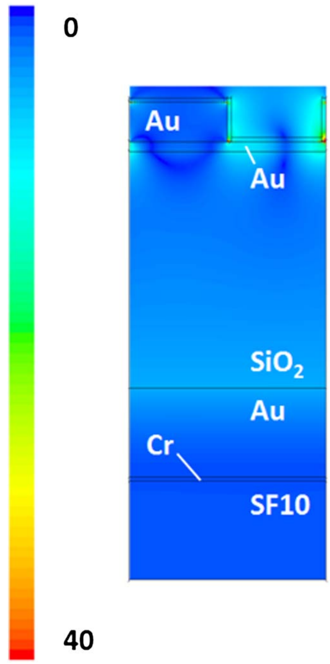

Fig. 7. FDTD results of the proposed LSPR structure at $d_D = 120$ nm and $d_{OL} = 5$ nm. The near-field distribution image of the E_X component is normalized by the field amplitude of 40.

contributes to a notable improvement of sensitivity via a stronger field–analyte interaction. An improved sensitivity for $d_{OL} = 5$ nm in Fig. 5 corroborates well with the enhanced maximum amplitude of the E_X field component obtained from the FDTD computation.

4. Conclusions

In summary, LSPR substrates with subwavelength gold nanogratings and MDM stack structure have been suggested to provide an enhancement in sensitivity and a high quality of SPR signal. Compared with a conventional SPR structure and a LSPR configuration without gold overlayer, the proposed LSPR structure leads to a large amplification of the SPR shift for a wide range of SiO_2 film thickness, possibly due to a higher subwavelength plasmon confinement and a longer propagation length. Moreover, the SPR signal quality and the dynamic range are significantly improved by the presence of a dielectric film and a gold overlayer, which is attributable to the nondestructive coupling between SP waves and LSP modes. The effects of MDM stack structure on the sensor performance are described by demonstrating the field distributions of the E_X component.

When the geometry of gold nanogratings is fixed at the period of $\Lambda = 100$ nm and a thickness of 20 nm and the chromium adhesion has a thickness of 2 nm, the optimal LSPR structure is determined as the MDM stack of $d_D = 110$ nm and $d_{OL} = 7$ nm. This LSPR substrate provides the highest SEF of 7.3 as well as a strong and deep absorption band at resonance. It is also worth emphasizing that the sensitivity of the proposed LSPR substrate can be significantly degenerated by an adhesion layer thicker than 5 nm. This design study could be helpful in optimizing the plasmonic substrate with metallic nanostructures and MDM stacks toward an improvement of sensor sensitivity and signal quality.

This research was supported by the Kyung Hee University Research Fund in 2012 (KHU-20120573).

References

1. J. N. Anker, W. P. Hall, O. Lyandres, N. C. Shah, J. Zhao, and R. P. Van Duyne, "Biosensing with plasmonic nanosensors," Nat. Mater. **7**, 442–453 (2008).
2. N.-H. Kim, W. K. Jung, and K. M. Byun, "Correlation analysis between plasmon field distribution and sensitivity enhancement in reflection- and transmission-type localized surface plasmon resonance biosensors," Appl. Opt. **50**, 4982–4988 (2011).
3. K. Kim, D. J. Kim, S. Moon, D. Kim, and K. M. Byun, "Localized surface plasmon resonance detection of layered biointeractions on metallic subwavelength nanogratings," Nanotechnology **20**, 315501 (2009).
4. S. M. Jang, D. Kim, S. H. Choi, K. M. Byun, and S. J. Kim, "Enhancement of localized surface plasmon resonance detection by incorporating metal-dielectric double-layered subwavelength gratings," Appl. Opt. **50**, 2846–2854 (2011).
5. W. P. Hu, S.-J. Chen, K.-T. Huang, J. H. Hsu, W. Y. Chen, G. L. Chang, and K.-A. Lai, "A novel ultrahigh-resolution surface plasmon resonance biosensor with an Au nanocluster-embedded dielectric film," Biosens. Bioelectron. **19**, 1465–1471 (2004).
6. R. F. Oulton, G. Bartal, D. F. P. Pile, and X. Zhang, "Confinement and propagation characteristics of subwavelength plasmonic modes," New J. Phys. **10**, 105018 (2008).
7. K. M. Byun, S. J. Kim, and D. Kim, "Design study of highly sensitive nanowire-enhanced surface plasmon resonance biosensors using rigorous coupled wave analysis," Opt. Express **13**, 3737–3742 (2005).
8. S. Elhadj, G. Singh, and R. F. Saraf, "Optical properties of an immobilized DNA monolayer from 255 to 700 nm," Langmuir **20**, 5539–5543 (2004).
9. E. D. Palik, *Handbook of Optical Constants of Solids* (Academic, 1985).
10. M. G. Moharam and T. K. Gaylord, "Rigorous coupled-wave analysis of metallic surface-relief gratings," J. Opt. Soc. Am. A **3**, 1780–1787 (1986).
11. Z. Liu, K.-P. Chen, X. Ni, V. P. Drachev, V. M. Shalaev, and A. V. Kildishev, "Experimental verification of two-dimensional spatial harmonic analysis at oblique light incidence," J. Opt. Soc. Am. B **27**, 2465–2470 (2010).
12. L. Li and C. W. Haggans, "Convergence of the coupled-wave method for metallic lamellar diffraction gratings," J. Opt. Soc. Am. A **10**, 1184–1189 (1993).
13. S. Ekgasit, C. Thammacharoen, F. Yu, and W. Knoll, "Influence of the metal film thickness on the sensitivity of surface plasmon resonance biosensors," Appl. Spectrosc. **59**, 661–667 (2005).